CPV and illumination systems based on XR-Köhler devices

Maikel Hernandez*[a], Aleksandra Cvetkovic[a], Pablo Benitez[a,b], Juan Carlos Miñano[a,b], Waqidi Falicoff[c], Yupin Sun[c], Julio Chaves[a], Ruben Mohedano[a]

[a]LPI-Europe, Edificio CEDINT, Campus de Montegancedo UPM, 28223 Pozuelo, Madrid, Spain
[b]CEDINT Universidad Politécnica de Madrid (UPM) ETSI Telecomunicación, C. Universitaria, 28040 Madrid, Spain
[c]LPI-LLC, Lincoln Ave., Altadena, CA 91001, USA

ABSTRACT

The XR-Köhler concentrator[1] is a design that has the possibility to work under high concentration, maintaining the high acceptance angle and high irradiance uniformity on the solar cell. It is an on-axis free-form design that consists of a reflective (X) and refractive (R) surface. For a geometrical concentration of about 800x the simulated results show an acceptance angle of ±1.79deg with high irradiance uniformity on the solar cell. This article shows the design results of the XR-Köhler and also a novel passive cooling system (LPI patented) that keeps the solar cell operation temperature under 100ºC at extreme conditions (wind speed = 0 m/s, module tilt angle = 45deg and T_a = 50ºC). The results of using the XR-Köhler device as a collimator when the light source has very high non-uniform luminance distribution, i.e. multichip LEDs, are also here presented.

Keywords: nonimaging, concentrator, photovoltaic, solar energy, free-form

1. INTRODUCTION

The use of multi-junction solar cells has made possible the increase of efficiency of concentration photovoltaic (CPV) systems. The use of multi-junction solar cells has also introduced new challenges in the development of the CPV systems because their high prices and their spectrum dependence. This means that high geometric concentration, C_g, is required, >500x, to minimize the impact of the solar cell cost on the system (as much as we increase the C_g, the impact of the cost of the solar cell on the system decreases). The increase of the C_g is limited by a thermodynamic limit [1] that can be expressed as follows:

$$CAP = \sqrt{C_g}\,\sin(\alpha) \le n \qquad (1)$$

Where *CAP* is the concentration-acceptance product [2], α is the acceptance angle (taking into account all optical losses) and *n* the refractive index of the material surrounding the solar cell. The advantage of using the *CAP* is that for a given concentrator architecture, the *CAP* keeps almost constant with C_g. This means that having the acceptance angle at a given concentration, the *CAP* can be used to estimate the acceptance angle that we would obtain if we design for a different concentration (for the same concentrator architecture). Maximizing α is the key to guarantee the success in maintaining the efficiency of CPV system when it is scaled from a single unit to array level. The acceptance angle measures the total tolerance available in the system for manufacturing and installation: optical elements quality, assembly, array installation, tracker stiffness and tracking accuracy. Having a higher α means that the system will be more tolerant to errors, it makes possible the decrease of the cost of energy produced by relaxing the accuracy of critical elements of the system.

[1] The LPI's XR-Köhler device presented in this paper is protected under US and International patents pending by LPI, LLC, 2400 Lincoln Avenue, Altadena, CA 91001 USA http://www.lpillc.com/.

The aforementioned equation shows the concentration-tolerance trade-off that the CPV systems developers have to face: reducing the cell cost impact by increasing the concentration and, at the same time, increasing the cost by reducing the system tolerance.
In this paper we will show the progress on the design of a XR-Köhler concentrator [3] by introducing a new degree of freedom in the design. It makes possible to raise the acceptance angle close to the XR SMS 3D [4] and XR SMS 2D [5] concentrators' acceptance angle. Here we also show a novel heat sink concept that will introduce a potential reduction in the manufacturing cost [6]. Finally, we show a preliminary evaluation of the potential of using the XR-Köhler device as a collimator when the light source is a multi-chip LED.

2. XR-KÖHLER CONCENTRATOR DESIGN

The XR-Köhler designs are based on four pairs of mirror and lens lenticulations, calculating the mirror as a generalized Cartesian oval instead of a parabola (see Figure 1). In this case we are substituting the parabolic primary by a free-form mirror, by modifying the spherical input wavefronts. As it will be shown, it gives the possibility to obtain designs that work close to the thermodynamic limit of concentration, and at the same time providing perfect uniformity on the receiver.

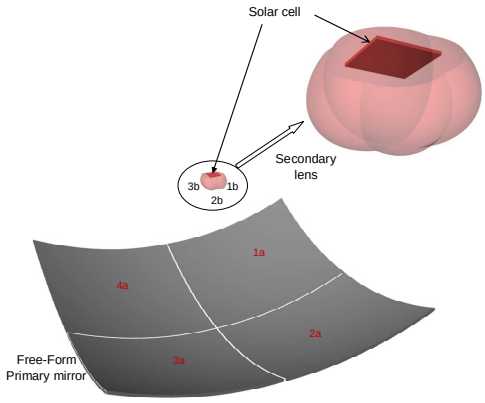

Figure 1. XR-Köhler concentrator geometry

Each lens is calculated as the Cartesian oval that couples two spherical wavefronts: one of them placed at the solar cell active area and the other one at the mirror. The criterion for placing such wavefronts is to maximize the uniformity of the irradiance distribution on the solar cell.

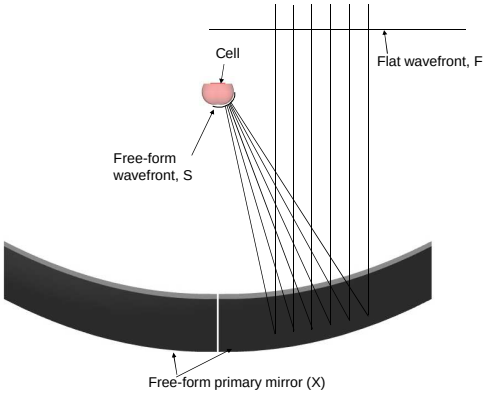

Figure 2. Wavefronts used to calculate the XR-Köhler mirror

The mirrors are calculated as a generalized Cartesian oval that couples a flat wavefront in one free-form (see Figure 2). Now the criterion for selecting these wavefronts is maximizing the optical efficiency when the concentrator is perfect aimed to the sun.

3. SIMULATION RESULTS FOR XR-KÖHLER CONCENTRATOR

In this section the comparison of different designs of XR-Köhler concentrator will be presented. The goal was to find the best performing design, analyzing the influence of the depth of the system on its performance. All designs are for 1cm^2 solar cell and 800cm^2 entry apertures. The influence of the depth of the system on acceptance angle, efficiency and peak irradiance has also been investigated. Several designs were carried out modifying the rim angle (θ in Figure 3). Finally the design that had the best acceptance angle was thoroughly analyzed.

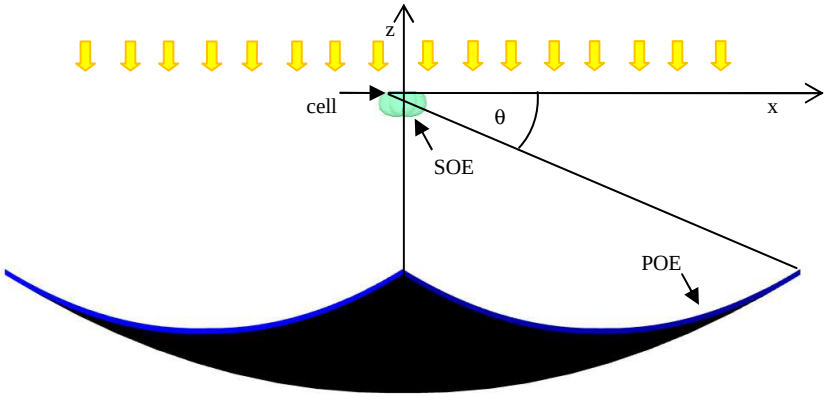

Figure 3. The parameter θ, used to optimize the XR-Köhler performance

To analyze the performance, the following ray-tracing parameters have been used: (i) POE is a silver coated mirror; (ii) SOE is made of B270 glass (n≈1.52) coupled to the cell with transparent silicone rubber of n≈1.41 (e.g., Sylgard 182 of Dow Corning); (iii) High efficiency (≈38%) commercial triple-junction cell, with the values of the external quantum efficiency provided by the manufacturer and considered to be independent of the incidence angle on the cell. Absorption in dielectric materials, Fresnel reflections losses and spectral transmission of materials are considered, but surface scattering is neglected. In monochromatic efficiency calculations is considered glass cover without anti-reflective coating of 91% of transmission and mirror of 95% of reflectance.

The behavior of the CPV system depends not only on solar-cell efficiency, but also on its sensitivity to spectral balance, due to the spectral selectivity of the junctions, variations in the spectra of the solar radiation and of the system's optical transfer function. Each component of the optical system has a spectrally dependent loss due to the Fresnel reflections losses and absorption by optical coatings. If the spectral transfer functions (*STFs*) are not balanced with the junction spectral response, photocurrent is 'starved' in one of the cells, reducing efficiency by holding the other two back.

For the simplification of the model we considered that the multi-junction cell behaves as three photodiodes connected in series, where each cell responds to a target slice of the solar spectrum. The photocurrent generated in the junction can be calculated according to:

$$I_i = \sum_{\lambda} A \frac{q \cdot Di(\lambda) \Delta\lambda \cdot \lambda}{h \cdot c} EQE(\lambda) \cdot \underbrace{T_{cover}(\lambda) \cdot T_{lens}(\lambda) \cdot R_{mirror}(\lambda)}_{STF(\lambda)} \qquad (2)$$

, where i=1, 2, 3, I_i is the photocurrent for the i-th junction, A is the cell area, q the electron charge, Di irradiance density ($Di(\lambda) = dP/dS \cdot d\lambda$, *i.e.* the power on the surface unit and for the unit wavelength [W/m·nm]), $EQE(\lambda)$, external quantum efficiency and h, Planck's constant.

The minimum current of the three diodes is chosen to approximate the electrical response of the solar cell. Figure 4 shows the spectral transmission curves for different optical elements of the XR-Köhler concentrator.

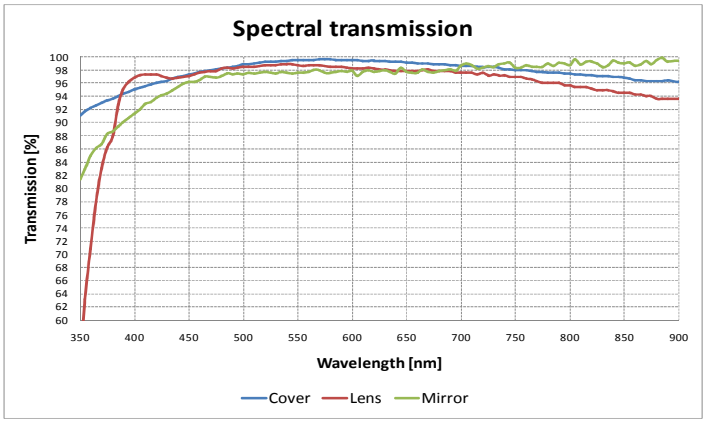

Figure 4. Spectral transmission curves for different optical elements of the XR-Köhler concentrator

If we define the optical efficiency as:

$$\eta = \frac{I_{sc(produced)}}{I_{sc(withoutlosses)}} \tag{3}$$

, where *Isc* are the short-circuit currents of the limiting sub-cell. For the XR-Köhler we obtained values of 81% (84.29% monochromatic) in the case without AR coating on the SOE and cover, and can reach 92.6% in the case with AR coatings.

3.1 Acceptance angle

One of merit functions used for the evaluation of the concentrator optical performance is the angular transmission of the concentrator, defined for a given incident beam of parallel rays as the power reaching the cell surface divided by the power incident on the concentrator aperture (i.e. the optical efficiency as a function of the angle of incidence of the parallel beam). The solar direct radiation is modeled as a set of parallel beams with the same radiance. The optical losses are considered in this computation. From the transmission curve we can determine the acceptance angle α, defined as the incidence angle at which the concentrator collects 90% of the on-axis power.
In the Figure 5 the variation of the acceptance angle for designs as function of the rim angle can be seen. This figure shows that the maximum acceptance angle has been obtained for a highly compact design with rim angle of 25º (what makes aspect ratio of this concentrator 0.4). Further analysis will be focused on the 25º rim angle design.

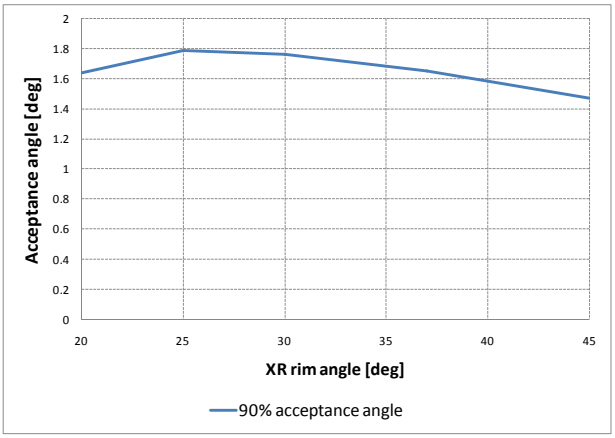

Figure 5. Concentrator of the acceptance angle for designs as function of the rim angle

The relative transmission curve of design for θ=25º is shown in Figure 6. The resulting XR-Köhler has C_g=800x achieving α= ±1.79 degrees.

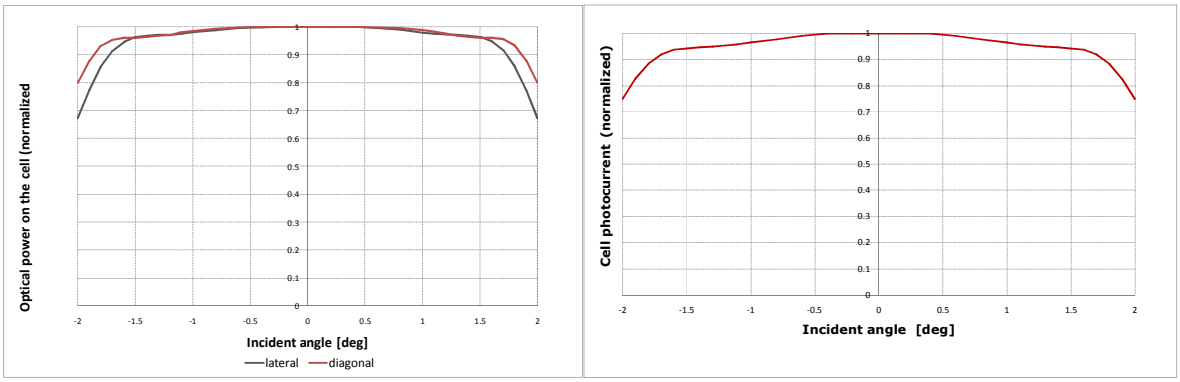

Figure 6. Left, relative transmission curves of XR-Köhler designed for θ=25 degrees. Right, photocurrent as function of the incidence angle

3.2 Irradiance and intensity on the cell

The analysis of irradiance distribution on the cell gives an excellent uniformity and the peak irradiance of 950 suns (@DNI 850W/m2). The irradiance on the cell is below 1000 suns, which is sufficiently low for present high-efficiency tandem solar cells. The simulation results of irradiance distribution on the cell when the concentrator is perfectly aimed to the sun can be seen in the Figure 7 (a).

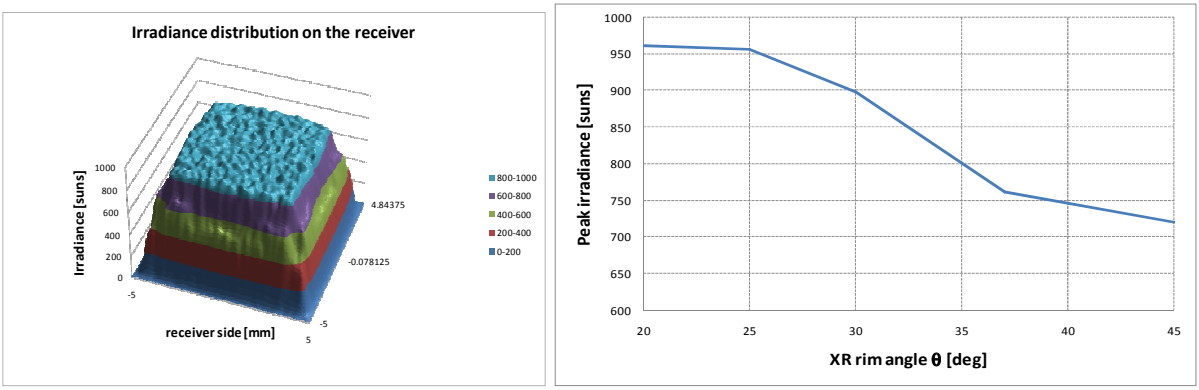

Figure 7. (a) Irradiance distribution on the cell when the concentrator is perfectly aimed, (@DNI 850W/m^2) (b) shows the peak irradiance on the cell versus rim angle θ for different XR-Köhler designs, all for concentration 800x. It can be seen that less compact designs have slightly lower peak irradiance on the cell, although all of them maintain it below 1000x

Another interesting feature is the angular intensity distribution of the light reaching the cell. Figure 8 shows the cumulative distribution of light power on the cell with off-normal angle. When the sun is perfectly tracked, the cell is entirely illuminated within a cone of ±50° or less from the solar cell normal. Since solar cell reflectivity is usually higher at large incidence angles (>50-60°) than at normal incidence, the intensity profile of the XR-Köhler concentrators guarantees optimum light coupling into the cell.

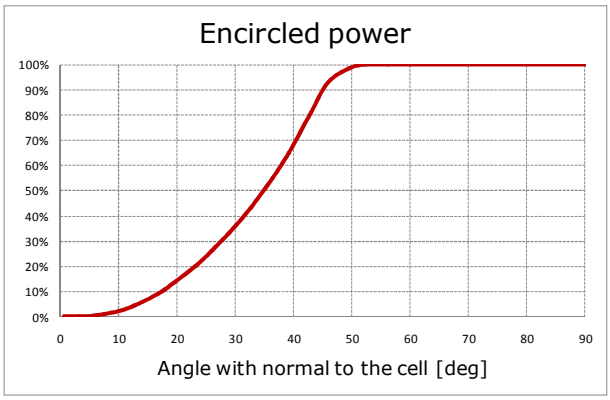

Figure 8. Cumulative distribution of light power received on the cell with off–normal angle for the XR-Köhler concentrator with parameters Cg=800x, θ=25º, when the sun is perfectly tracked

3.3 Tolerance study

In CPV systems it is very important to have high tolerances in in-fab assembly or in field installation, because it directly influences on the performance of the whole system. We have analyzed influence on the system performance in the case of misalignment among optical elements, considering lateral and vertical displacement, and twist of receiver with SOE respect to the POE (as shown in Figure 9). The influence of the misalignments has been analyzed on the following merit functions:

1) Optical efficiency
2) Acceptance angle (half-angle)
3) Peak irradiance (maximum irradiance at cell active surface).

For all calculations we have used an extended light source with the same angular spread as the sun.

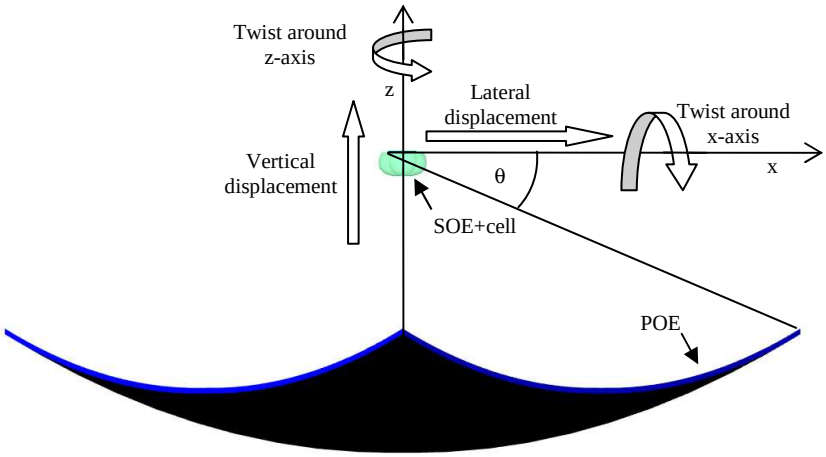

Figure 9. Analyzed tolerances description: Lateral and vertical displacements and twist of receiver with SOE respect to the POE

Next Table shows the summary of tolerance analysis. For the acceptance angle the most critical error is vertical displacement (see Figure 10), since it drops from 1.79º to 0.9º for 5mm error. Also is significant the decrement of acceptance angle for the rotational error of SOE when the acceptance angle gets bellow 1º for twists of 13º. In the case of peak irradiance on the cell, it can be kept below the maximum value for the multi-junction solar cells (about 1500 suns), for all analyzed positioning errors, thus the lateral displacement of SOE+cell of 5mm increases the peak irradiance in the cell to 1424x.

Tolerances SOE+receiver					
		Displacement		Twist	
	Nominal values	Lateral displacement	Vertical displacement	Around x-axis	Around z-axis
Acceptance angle	1.79º	±5mm: 1.56º	-5mm: 1.27º +5mm: 0.9º	±15º: 0.7º	±20º: 1.16º
Peak irradiance	935x	±5mm: 1424x	-5mm: 1062x +5mm: 858x	±15º: 1150x	±20º: 1020x
Efficiency	82.7%	±5mm: 78.3%	-5mm: 82.6% +5mm: 81.8%	±15º: 75.2%	±20º: 79.8%

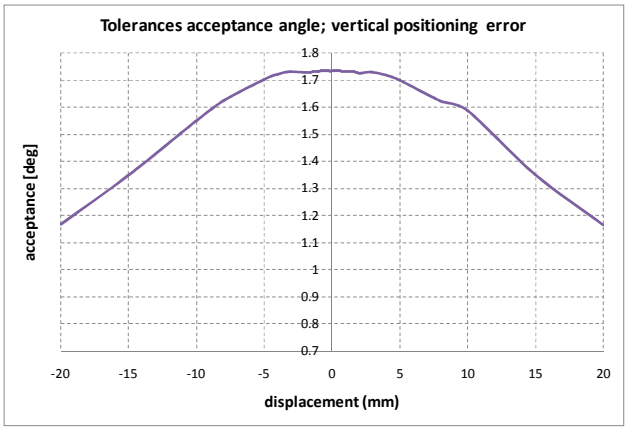

Figure 10. Acceptance angle dependence on the vertical receiver vertical displacements

4. ON-WINDOW SOLAR CELL HEAT SPREADER

In concentrating and collimating optoelectronic applications, it is in general necessary to extract heat from the optoelectronic device (LED, laser, solar cell). For that purpose a metallic heat spreader is usually needed. In the case of a Cassegrain (rear-focus) location, the heat spreader can have radiator fins attached to it to transfer the heat to the ambient environment (usually the atmosphere) behind the primary mirror. The width of the optoelectronic device is typically small compared to that of the aperture but the attached heat sink is not. That is because the area needed to transfer the heat generated at the optoelectronic device to the ambient at a reasonable temperature drop is typically of similar area to the aperture itself. The fins increase the area without increasing too much the heat sink volume, but still the heat sink is usually comparable in size with the optics aperture.

As a solution we propose a special transparent cover across the aperture of a reflective concentrator or collimator, such that the heat of the optoelectronic device is spread across the cover [6]. Once spread, the heat can easily flow to the ambient with a reasonable temperature drop even though glass and other commonly used cover materials do not have good thermal conductivity. This is so because the heat flow area has been increased enough to exhibit a low thermal resistance to the heat flow. A 6 mm thickness of glass will conduct 166 Watts/m2 when there is a 1°C temperature difference from one face to the other of the glass, if the heat is flowing directly through the glass. Thus the 65% heat generation of a high-efficiency solar cell will require a 4°C difference at one sun (1000 Watts/m2), which is a very small temperature drop.

The special cover is formed by a glass with thin strips of thermally conductive material radiating out from the reflector focus in order to spread the target's heat over the glass cover, termed the Heat-Spreading Transparent Cover (HSTC). Because the heat must spread laterally over the glass, as well as through it, the average temperature drop from the metal strips to the external atmosphere will be more than the 1 °C per 6 mm calculated above, and will depend on how far apart the strips are.

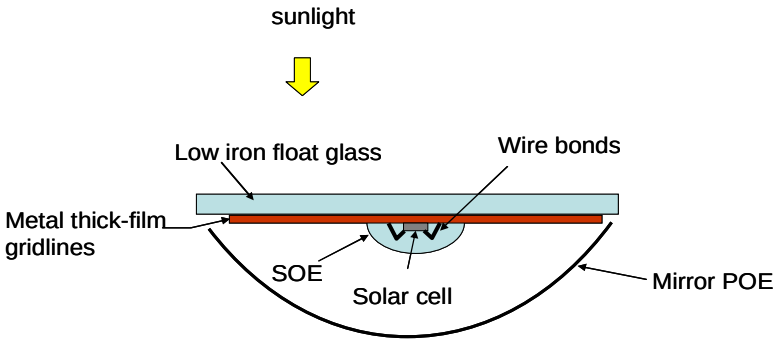

Figure 11. Description of the heat sinking concept

The strips can be electrically conductive, providing vias for a multiplicity of requirements, or can form hollow vias within which separate wiring, electrically insulated from the strips themselves. For example, the strips can be used to connect an array of PV cells in series, or can be bonded to the front cover using an adhesive that is reflective to sunlight to mitigate heat buildup due to absorption. The deep strips can also be highly specularly reflective to reduce heat buildup but also to redirect grazing incidence rays to the primary mirror or optic and in the reverse direction to the target. These mirrored vertical strips would interfere minimally with the working of the concentrator, since they follow the flow-lines of the incoming radiation.

The solar concentrator in Figure 11 is composed of solar cell mounted on a base, spreader bars or strips radiating from base, and secondary lens covering the cell. Base with spreader bars, cell and secondary lens, is mounted on the inside of cover glass, which is faced by primary reflector. For the calculation we used small sized system where the primary reflector is 50 mm on a side and secondary lens is 10 mm in diameter and solar cell of 2.24 mm side. Spreader bars are 0.5 mm wide. Base and spreader bars have a depth of 0.6 mm and are made of copper (or some other suitable highly conductive material).

In spite of the fierce concentration (geometrical concentration 500 suns) onto chip a cell delta temperature only 50°C above ambient can be achieved. Other assumptions include: the solar radiation at the location is 850W/m2, module tilt angle is 45ºC, wind speed is 0 m/s, the optical efficiency is 80%, the PV cell efficiency is 31% (a conservative figure), and the cover is common glass 6 mm thick. In that implementation, 1.175 W of heat must be dissipated from the cover. This is a direct benefit of the relatively small size of this system, which encourages arraying. In this case the loss due to the shadowing is only 7%, what is comparable with losses of traditional systems that have more complex, larger, and more expensive heat sink, where loss is about 5%.

Figure 12 shows a view of the array of concentrators similar to that of Figure 11, assembled but with side walls and supports not shown.

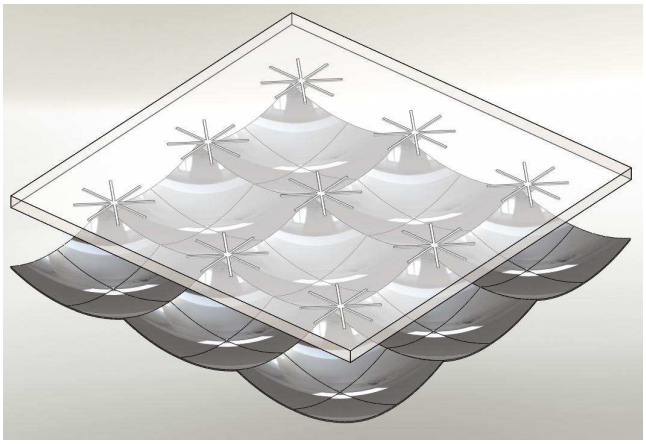

Figure 12. Description of the module concept

5. XR-KÖHLER FOR ILLUMINATION

In commercially available LEDs the emitters have sharp spatial variations in luminance caused by wire bonding shadowing or because they are composed by several chips leaving in the areas between them low luminance or even dark areas. The next picture shows the CREE´s XLamp® MP-L EasyWhite™ LED which is a very good example of a multi-chip white LED.

Figure 13. CREE's XLamp® MP-L EasyWhite™ LED

We run some simulations in order to do a preliminary evaluation of the XR-Köhler device ability of creating a uniform intensity pattern from such LEDs. This design is not optimized for illumination but for photovoltaic, however it is a good exercise to see if this device has potential use as collimator. The following picture shows how the XR-Köhler (with XLamp LED and a spherical cavity on the secondary optical element) creates a highly uniform intensity pattern: (left) black and white linear scale 2D pattern, (right) section of the intensity pattern.

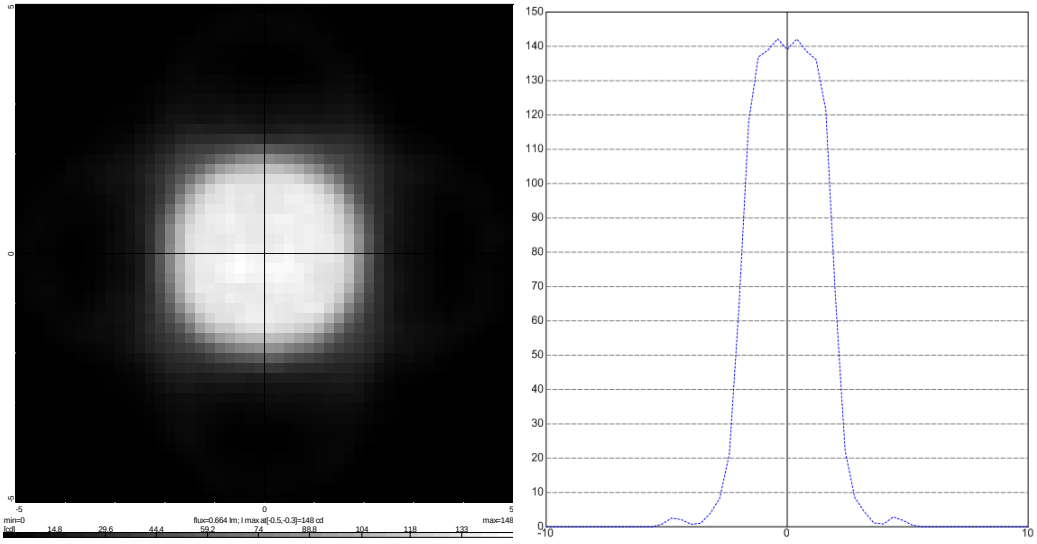

Figure 14. XR-Köhler (with XLamp LED a spherical cavity on the secondary optical element):left, black and white linear scale 2D pattern, right, section of the intensity pattern

We also traced the XR-Köhler device with a warm white LED that combines LEDs from different colors (Figure 15 left) to qualitatively evaluate the XR-Köhler mixing color properties. In the intensity pattern, (Figure 15 right), can be seen that the optical device creates a high uniform and no visible color separation pattern. However there is a visible color separation near the corners which indicates that for mixing color application more complex design would be needed: more lenticulation pairs, cavity design or both.

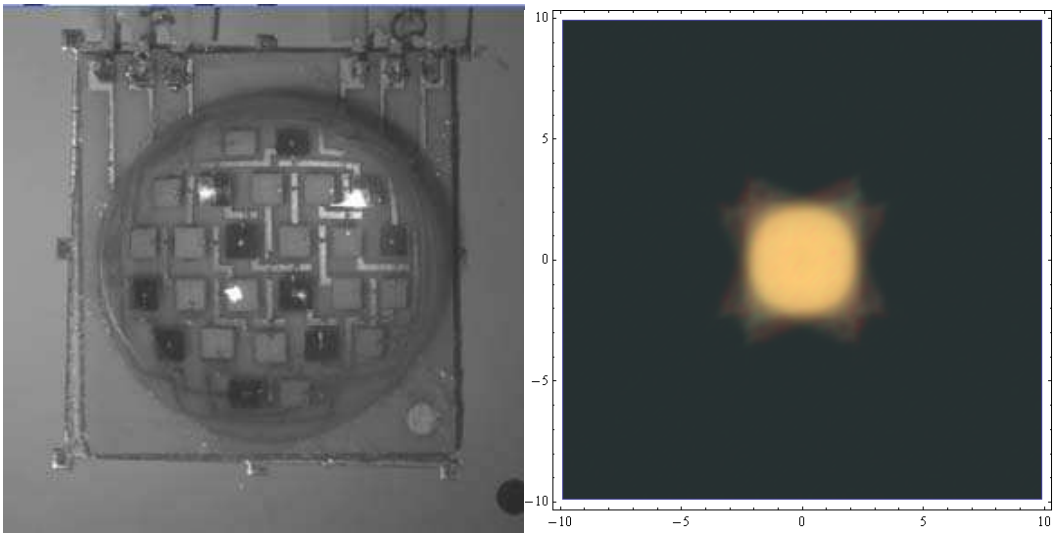

Figure 15. XR-Köhler (with XLamp LED a spherical cavity on the secondary optical element):left, black and white linear scale 2D pattern, right, section of the intensity pattern.

6. CONCLUSIONS

A new XR-Köhler concentrator was designed optimizing not only the irradiance on the solar cell but also its acceptance angle. Acceptance angle of ±1.79deg (for 800x of geometric concentration) has been obtained by introducing new degrees of freedom on the design. The XR-Köhler concentrator has also high optical efficiencies with and without AR coating, 92.6% and 81.0% respectively. This performance results are comparable to the one obtained with other XR based concentrators, like XR SMS 3D and the XR SMS 2D. We also have shown that the XR-Köhler concentrator is highly tolerant to positioning errors.
We also presented a novel heat sinking concept that keeps the solar cell operation temperature under 100ºC at extreme conditions (wind speed = 0 m/s, module tilt angle = 45deg and Ta = 50ºC).

Finally, we show the potential use of the XR-Köhler device as a collimator when the light source is a multi-chip LED or similar. This application requires more refinement but the preliminary results are very promising.

ACKNOWLEDGMENTS

Support for this work partly comes from the EC and Spanish Ministry MICINN under projects SSL4EU, 257550, FP7-ICT-2009-5 and SIGMASOLES PSE-440000-2009-8, respectively.

REFERENCES

[1] Winston, R., Miñano J.C., Benítez P., "*Nonimaging optics*", (Elsevier-Academic Press, New York, 2005

[2] Benitez P., Miñano J. C., "*Concentrator Optics for the next generation photovoltaics*". Chap. 13 of A. Marti & A. Luque. Next Generation Photovoltaics: High Efficiency through Full Spectrum Utilization, (Taylor & Francis, CRC Press, London, 2004).

[3] Hernández, M., Cvetkovic, A., Benítez, P., Miñano, J. C., "*High-performance Köhler concentrators with uniform irradiance on solar cell*" in Nonimaging Optics and Efficient Illumination Systems V, edited by Roland Winston, R. John Koshel, Proceedings of SPIE Vol. 7059 (SPIE, Bellingham, WA 2008) 705908

[4] Cvetković, A., Hernandez, M., Benítez, P., Miñano, J. C., Schwartz, J., Plesniak, A., Jones, R., Whelan, D., "*The SMS3D photovoltaic concentrator*" in Nonimaging Optics and Efficient Illumination Systems V, edited by Roland Winston, R. John Koshel, Proceedings of SPIE Vol. 7059 (SPIE, Bellingham, WA 2008) 705909

[5] Hernández, M., Benítez, P., Miñano, J. C., Cvetkovic, A., Mohedano, R., Dross, O., Jones, R., Whelan, D., Kinsey, G. S., Alvarez, R., "*XR: a high-performance PV concentrator*" in High and Low Concentration for Solar Electric Applications II, edited by Martha Symko-Davies, Proceedings of SPIE Vol. 6649 (SPIE, Bellingham, WA 2007) 664904

[6] US and International patents and patents pending, including: 7,460,985, US 2008/0223443, US 2008/0316761